URSI AP-RASC, Sydney, Australia, 17 – 22 August 2025

Kernel Regression for Predicting Magnetic Field Distributions in Railway Catenary Systems

N. Soleimani(1), G. M. Monteverde(1), B. Cintolesi(1), P. Piccardo(1), F. Fichera(1), C. Coladonato(1), R. Trinchero(2)
(1) Hitachi Rail
(2) Politecnico di Torino, Turin, Italy

Abstract

This paper presents a machine learning approach to predict the magnetic field distribution in railway catenary systems. The proposed method leverages kernel regression to account for tolerances in system parameters. The accuracy of the model is assessed by comparing predicted fields to ground-truth data obtained via the Biot-Savart equation. Results demonstrate the effectiveness of the method with different training sample size.

1 Introduction

A catenary system is a crucial component of electrified railway infrastructure, consisting of overhead wires that deliver electrical power to trains. These systems are designed to maintain reliable electrical contact between the train's pantograph and the power supply, even under dynamic conditions. The catenary system includes the contact wire, messenger wire, and droppers, which together ensure mechanical stability and efficient power transfer. Given their proximity to trains and passengers, understanding the electromagnetic behavior of these systems is vital for safety, system design, and electromagnetic compatibility (EMC) [1]–[4].

Predicting the magnetic field distribution in railway catenary systems is essential due to its implications for operational safety and regulatory compliance. Electromagnetic fields must adhere to stringent EMC standards, such as the EN 50500 [5], limiting magnetic field values to mitigate interference and health risks [1, 2]. Accurate modeling of these fields is critical, due to the effect of system tolerances and uncontrolled variations, such as: deviations in wire geometry, current magnitudes, antenna positions, site configuration, and environmental conditions [2, 3].

This work investigates the ability of kernel regression techniques to approximate magnetic field distributions under varying system configurations. Specifically, the vector-valued kernel ridge regression (VV-KRR) [6, 7] is employed to learn the magnetic field map of the catenary system as a function of 16 uniformly distributed parameters. The methodology is validated through numerical simulations based on a simplified model using the Biot-Savart law, demonstrating its effectiveness and accuracy with different training sample sizes. The results underscore the potential of data-driven models to enhance electromagnetic analysis in railway applications, contributing to improved system design and compliance with EMC standards.

It is worth noting that, while the Biot-Savart law serves as an effective tool for demonstrating the applicability and the effectiveness of the proposed machine learning techniques in this context, the data-driven nature of the proposed modeling framework also enables it to approximate results obtained from more sophisticated simulation techniques and advanced models [3, 4].

2 Proposed Method

The proposed method for predicting the magnetic field distribution in railway catenary systems combines the efficiency of the Biot-Savart law with the power of machine learning for generalizing across various configurations. In the following subsections, we discuss the two key components of the method: the magnetic field estimation using the Biot-Savart law and the kernel regression model used for field prediction across different system configurations.

2.1 Magnetic Field Estimation Using the Biot-Savart Law

For N wires located along the z-axis and placed in the (x,y)-plane at the position $(x_{s,i}, y_{s,i})$ each of them carrying a constant current $I_{s,i}$, the magnetic field components $(B_x(x,y), B_y(x,y))$ at any field point $(x,y) \neq (x_{s,i}, y_{s,i})$ calculated using the Biot-Savart law are expressed as:

$$B_x(x,y) = \frac{\mu_0}{4\pi} \sum_{i=1}^{N} I_{s,i} \frac{-(y-y_{s,i})}{(x-x_{s,i})^2 + (y-y_{s,i})^2}, \tag{1}$$

and

$$B_y(x,y) = \frac{\mu_0}{4\pi} \sum_{i=1}^{N} I_{s,i} \frac{x-x_{s,i}}{(x-x_{s,i})^2 + (y-y_{s,i})^2}. \tag{2}$$

in which μ_0 is the permeability of free space.

The above equations have been implemented in MATLAB by considering a discrete grid of equally spaced points in the (x,y)-plane. Specifically, after the discretization of the domain, the continuous variables x and y in equations (1) and (2) are replaced by the discrete variables

$x_j = x_0 + \Delta_x \cdot j$ and $y_k = y_0 + \cdot \Delta_y \cdot k$, with $j = 0 \ldots (N_x - 1)$ and $k = 0 \ldots (N_y - 1)$, respectively.

The magnitude of the magnetic field B for any pair (x_j, y_k) writes:

$$B(x_j, y_k) = \sqrt{B_x^2(x_j, y_k) + B_y^2(x_j, y_k)}. \tag{3}$$

To avoid numerical instability induced by the spatial discretization, the magnitude of the magnetic field B in (3) is considered 0, when the distance of a discrete point (x_j, y_k) from any source point $(x_{s,i}, y_{s,i})$ is less than Δ_x along the x-dimension and Δ_y along the y-dimension, respectively.

It is important to remark that the proposed method predicts a quasi-static DC solution (i.e., it does not account for propagation and frequency-dependent effects), assuming ideal and infinitely long straight conductors with negligible radius [4]. On the other hand, thanks to its high efficiency and low computational cost, the proposed implementation of the Biot-Savart law offers a valid and interesting approach for benchmarking machine learning techniques.

For higher accuracy more sophisticated methods, such as those based on the multiconductor transmission line theory [3, 4], can be employed. These approaches, though computationally more demanding, can provide more accurate results by considering factors such as wire geometry, frequency-dependent propagation effects, and the influence of nearby materials.

2.2 Kernel Regression for Magnetic Field Prediction

The VV-KRR can be employed for the prediction of the magnetic field distribution of a catenary system as a function of the positions of the catenary cables and the magnitude of their currents. For a fixed value of the discretization variables Δ_x and Δ_y, and number of discrete points N_x and N_y, the problem is equivalent of building an approximation $\hat{\mathbf{F}}$ of the following matrix of functions:

$$\mathbf{B}(\boldsymbol{x}_s, \boldsymbol{y}_s, \boldsymbol{I}_s) \approx \hat{\mathbf{F}}(\boldsymbol{x}_s, \boldsymbol{y}_s, \boldsymbol{I}_s), \tag{4}$$

where for each configuration of the source parameters in the vectors $\boldsymbol{x}_s$, $\boldsymbol{y}_s$ and $\boldsymbol{I}_s$, the output $\mathbf{B}(\boldsymbol{x}_s, \boldsymbol{y}_s, \boldsymbol{I}_s)$ is a $(N_x \times N_y)$ matrix function, hereafter referred to as computational model, collecting the actual values of the B-field computed via the Biot-Savart law described in the previous subsection. On the other hand, $\hat{\mathbf{F}}$ is an approximated model, hereafter referred to as surrogate model.

In this work the surrogate model will be build via the VV-KRR. To this aim, the above matrix learning problem is rewritten in term of the following equivalent vector problem:

$$\text{vec}\left(\mathbf{B}(\boldsymbol{x}_s, \boldsymbol{y}_s, \boldsymbol{I}_s)\right) \approx \hat{\boldsymbol{f}}(\boldsymbol{x}_s, \boldsymbol{y}_s, \boldsymbol{I}_s), \tag{5}$$

where now $\text{vec}\left(\mathbf{B}(\boldsymbol{x}_s, \boldsymbol{y}_s, \boldsymbol{I}_s)\right)$ and $\hat{\boldsymbol{f}}$ are vectors functions with $(N_x \cdot N_y)$ elements each.

The VV-KRR model is built starting from a set training samples $\mathcal{D} = \{(\tilde{\boldsymbol{x}}_l, \boldsymbol{y}_l\}_{l=1}^{L}$, where the vectors $\tilde{\boldsymbol{x}}_l = [\boldsymbol{x}_{s,l}, \boldsymbol{y}_{s,l}, \boldsymbol{I}_{s,l}]^T \subseteq \mathbb{R}^p$ collect the configurations of p input parameters, and the vectors $\boldsymbol{y}_l = \text{vec}\left(\mathbf{B}(\boldsymbol{x}_{s,l}, \boldsymbol{y}_{s,l}, \boldsymbol{I}_{s,l})\right) \subseteq \mathbb{R}^D$ of dimension $D = (N_x \cdot N_y)$ collect the B-field values calculated for the considered discrete points along x and y. The above training set can be used to train a surrogate model via the VV-KRR [6, 7], in the form of:

$$\hat{\boldsymbol{f}}(\tilde{\boldsymbol{x}}) = \sum_{l=1}^{L} \mathbf{K}(\tilde{\boldsymbol{x}}, \tilde{\boldsymbol{x}}_l) \boldsymbol{c}_l, \tag{6}$$

where $\mathbf{K}(\cdot,\cdot) : \mathbb{R}^{p \times p} \to \mathbb{R}^{D \times D}$ is the matrix kernel function and $\boldsymbol{c}_l = [c_{1,l}, \ldots, c_{N_x \cdot N_y, l}]^T$ for $l = 1, \ldots, L$ are column vectors collecting the regression unknowns, which must be estimated during the training phase.

According to [8], the separable kernel matrix $\mathbf{K}(\mathbf{x}, \mathbf{x}')$ can be expressed as follows:

$$\mathbf{K}(\tilde{\boldsymbol{x}}, \tilde{\boldsymbol{x}}') = k_{\boldsymbol{x}}(\tilde{\boldsymbol{x}}, \tilde{\boldsymbol{x}}') \mathbf{B}, \tag{7}$$

where $k_{\boldsymbol{x}}(\tilde{\boldsymbol{x}}, \tilde{\boldsymbol{x}}')$ is a standard scalar kernel acting on the input parameters and $\mathbf{B} \in \mathbb{R}^{(N_x \cdot N_y) \times (N_x \cdot N_y)}$ is a symmetric semi-definite matrix built from the correlation matrix computed on the output dimension of the output samples in the training set.

The separable kernel structure of the matrix kernel in (7) allows reformulating the training problem in terms of the following discrete-time Sylvester equation [6, 7]:

$$\mathbf{K}_{\boldsymbol{x}} \mathbf{C} \mathbf{B} + \lambda \mathbf{C} = \mathbf{Y}, \tag{8}$$

where $\mathbf{K}_{\boldsymbol{x}}$ is a $L \times L$ Gram matrix of the input kernel (i.e., $[\mathbf{K}_{\boldsymbol{x}}]_{ij} = k_{\boldsymbol{x}}(\boldsymbol{x}_i, \boldsymbol{x}_j)$), $\mathbf{B}$ is the the output kernel defined as the correlation matrix computed on the output dimensions, $\mathbf{C} = [\boldsymbol{c}_1, \ldots, \boldsymbol{c}_L]^T \in \mathbb{R}^{L \times D}$ is a matrix collecting the model unknowns and $\mathbf{Y}$ is the $L \times D$ matrix associated to the training output samples [8].

The surrogate model in (8) is then constructed from the training set $\mathcal{D}$ by solving the above discrete-time Sylvester equation via the efficiency diagonalization procedure presented in [9].

3 Results

This section investigates the performance of the proposed VV-KRR for the prediction of the magnetic B-filed in a catenary system with 8 sources, as a function of a uniform and uncorrelated variations of their current amplitude and the position of the contact and messenger wires. Table 1 summarizes the configurations of the considered parameters and the corresponding range of variation used in the following results. The above scenario is modeled in terms of 16 normalized uniform distributed random variables.

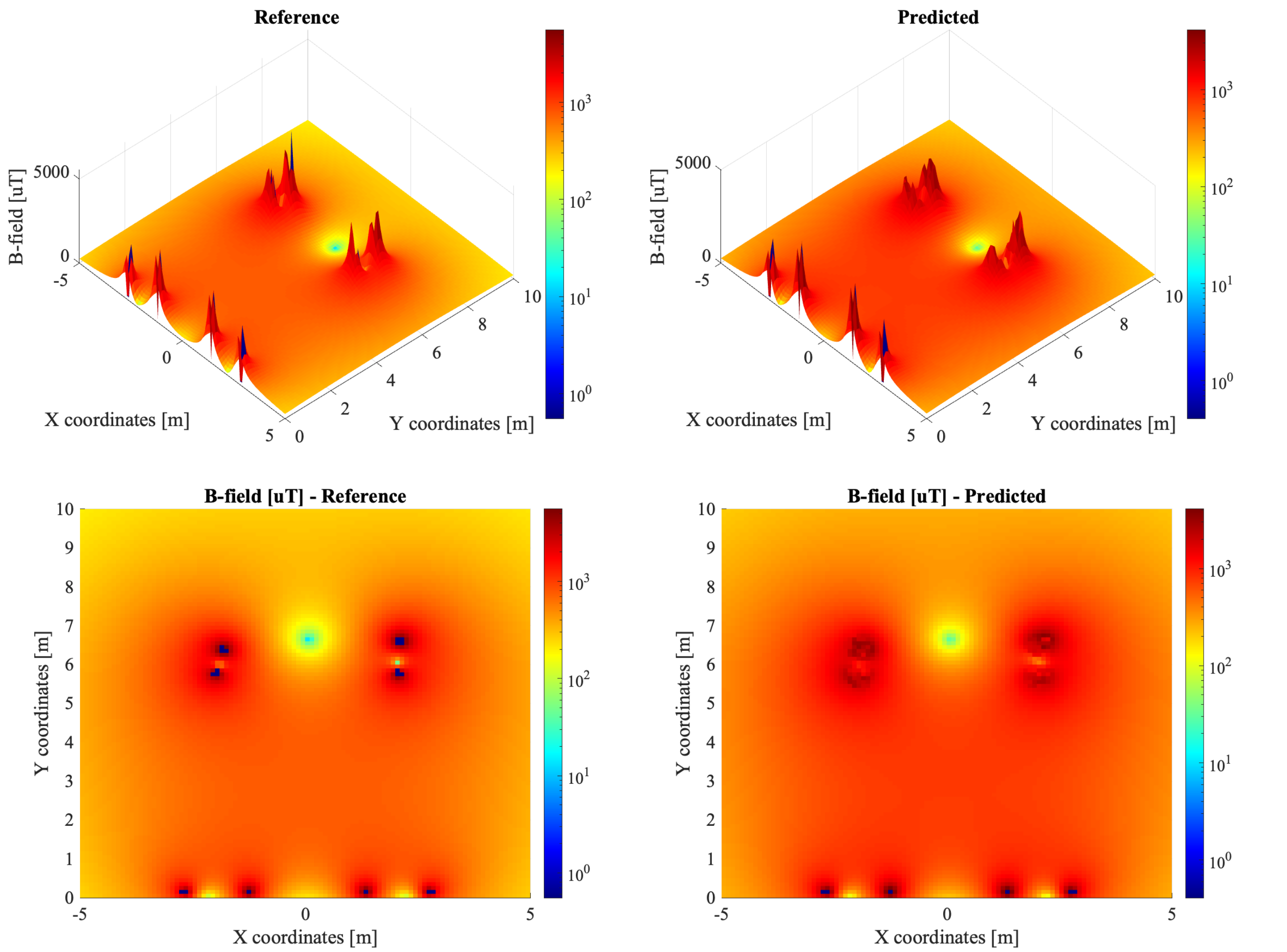

Figure 1. Comparison of the magnitude of the B-field computed via the Biot-Savart law for a given configuration of the sources and the corresponding prediction of a surrogate model trained with $L = 300$ training samples.

Table 1. Relative Mean Error for Varying Training Sizes

Source #	x_s	y_s	I_s
1	1.3m	0.1m	[1868,2068]A
2	2.7m	0.1m	[1354,1554]A
3	[1.8,2.2]m	[5.4,5.8]m	[-1980,-1780]A
4	[1.8,2.2]m	[6.2,6.6]m	[-2920,-2720]A
5	-2.7m	0.1m	[1354,1554]A
6	-1.3m	0.1m	[1868,2068]A
7	[-2.2,-1.8]m	[5.4,5.8]m	[-1980,-1780]A
8	[-2.2,-1.8]m	[6.2,6.6]m	[-2920,-2720]A

The MATLAB implementation of the Biot-Savart law presented in Sec. 2.1 is then used as a reference method to compute the B-filed of the considered parametrized catenary system in the xy-plane for $x \in [-5,5]$ m and $y \in [0,10]$ m by considering a discretization step $\Delta_x = \Delta_y = 0.1$ m. This means that for each configuration of the parameters the MATLAB implementation provides a 200×101 matrix $\mathbf{B}(\boldsymbol{x}_s, \boldsymbol{y}_s, \boldsymbol{I}_s)$ (i.e., $N_x = 200$ and $N_y = 101$).

The above MATLAB configuration is then used to run 800 parametric simulations. The obtained results for the B-filed are then vectorized and used as reference output samples to train and to validate the proposed modeling approach.

The VV-KRR presented in Sec. 2.2 is then used to train a surrogate model $\hat{\boldsymbol{f}} : \mathbb{R}^{16} \to \mathbb{R}^{20200}$, being $20200 = (N_x \cdot N_y)$ the number of outputs required to describe the B-filed after the vectorization. The performance of the resulting surrogate models has been investigated for an increasing number of training samples randomly selected from the available samples, and the performance of the resulting models are then evaluated on the same test set with 200 samples.

Table 2 summarizes the accuracy using the relative mean absolute error (RMAE) compute on the test samples by comparing the actual B-filed map with the predictions obtained by the proposed machine learning model trained with $L = 100$, 300 and 600 training samples. The table shows a constant learning of the model since the model error monotonically decreases when the number of training samples increases.

Figure 1 provides a visual comparison of the magnitude of

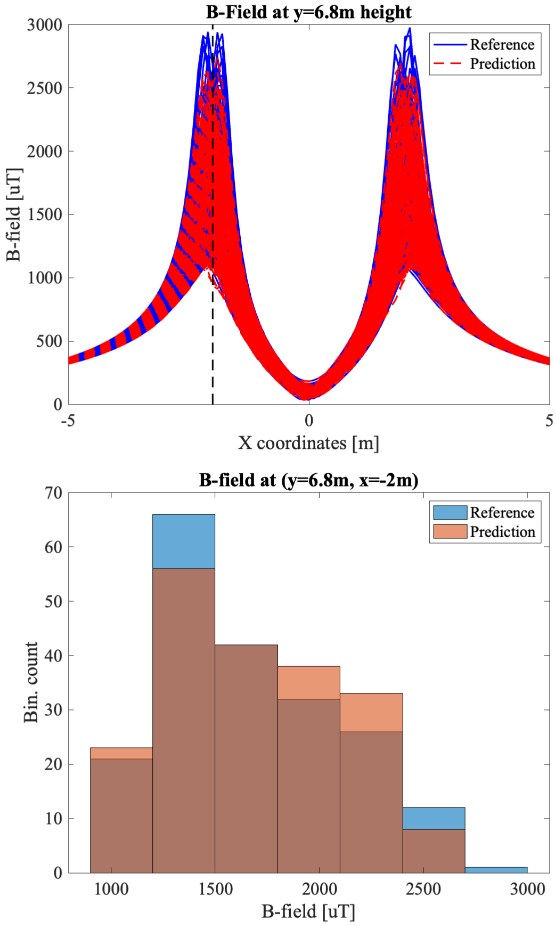

Figure 2. Top panel: parametric plots comparing B-filed predicted by the proposed model trained with 300 samples with the corresponding values in the test set at the heigth $y = 6.8\,\mathrm{m}$. Bottom panel: histogram obtained from the results of the above parametric plot for $x = -2\,\mathrm{m}$.

the B-field computed via the Biot-Savart law (i.e., the reference result) for a given configuration of the sources and the corresponding prediction of a surrogate model trained with $L = 300$ training samples. The proposed comparison in terms of 3D plot and 2D field map highlights a quite nice agreement between the predictions of the model and the reference results. Moreover, figure 2 provides a comparison among the values of the magnetic field in the test set and the corresponding predictions at fixed height ($y = 6.8\,\mathrm{m}$) and for different position on the x-axes, and the corresponding histogram for $x = -2\,\mathrm{m}$. The results provides a further confirmation of the model accuracy from both the deterministic and stochastic perspective.

4 Conclusion

This paper demonstrated the effectiveness of kernel regression for predicting magnetic fields in catenary systems. The approach shows promising results in terms of accuracy both in the deterministic and statistical sense. Future work will extend this method to more complex geometries and parameter variations.

Table 2. RMAE for varying training sizes.

Training Samples	RMAE (%)
L=100	2.1
L=300	1.7
L=600	1.5

References

[1] A. Mariscotti, "Normative Framework for the Assessment of the Radiated Electromagnetic Emissions from Traction Power Supply and Rolling Stock," 2019 IEEE Vehicle Power and Propulsion Conference (VPPC), Hanoi, Vietnam, 2019, pp. 1-7.

[2] A. Mariscotti, "Critical Review of EMC Standards for the Measurement of Radiated Electromagnetic Emissions from Transit Line and Rolling Stock", *Energies*, 2021.

[3] A. Cozza and B. Demoulin, "On the Modeling of Electric Railway Lines for the Assessment of Infrastructure Impact in Radiated Emission Tests of Rolling Stock," in *IEEE Transactions on Electromagnetic Compatibility*, vol. 50, no. 3, pp. 566-576, Aug. 2008.

[4] B. Cintolesi, et al, "Modeling the magnetic field emissions from a third rail system," Electrical Systems for Aircraft, Railway and Ship Propulsion, Bologna, Italy, 2010, pp. 1-5.

[5] CEI, "Measurement procedures of magnetic field levels generated by electronic and electrical apparatus in the railway environment with respect to human exposure," CEI EN 50500, 2014.

[6] A. Mauricio, L. Rosasco, and N. D. Lawrence, "Kernels for vector-valued functions: A review," *Foundations and Trends in Machine Learning* 4(3) pp. 195-266, 2012.

[7] N. Soleimani, R. Trinchero and F. Canavero, "Bridging the Gap Between Artificial Neural Networks and Kernel Regressions for Vector-Valued Problems in Microwave Applications," *IEEE Transactions on Microwave Theory and Techniques*, vol. 71, no. 6, pp. 2319-2332, June 2023.

[8] N. Soleimani, et al, "Vector-Valued Kernel Ridge Regression for the Modeling of the Scattering Parameters of a Slotted Ground PCB Structure," 4th URSI AT-RASC, Meloneras, Spain, 2024, pp. 1-4.

[9] N. Soleimani and R Trinchero, "Efficient Implementation of the Vector-Valued Kernel Ridge Regression for the Parametric Modeling of the Frequency-Response of a High-Speed Link," XXXVth URSI GASS, Sapporo, Japan, 2023, pp. 1-4.